Chapter 4

Basic of SFRA

4.1 Introduction

Sweep Frequency Response Analysis (SFRA) is a tool that can give an indication of core or winding movement in transformers. This is done by performing a measurement, a simple one, looking at how well a transformer winding transmits a low voltage signal that varies in frequency. Just how well a transformer does this is related to its impedance, the capacitive and inductive elements of which are intimately related to the physical construction of the transformer. Changes in frequency response as measured by SFRA techniques may indicate a physical change inside the transformer, the cause of which then needs to be identified and investigated. In order to understand the practical implementation of SFRA, at first, basic theory of SFRA has to be explained in detail and same is the objective of this chapter.

4.2 Circuit Theory of SFRA

The primary objective of SFRA is to determine how the impedance of a test specimen behaves over a specified range of applied frequencies. The impedance is a distributed network of active and reactive electrical components. The components are passive in nature, and can be modeled as resistors, inductors, and capacitors. The reactive properties of a given test specimen are dependent upon and sensitive to changes in frequency. The change in impedance versus frequency can be dramatic in many cases. This behavior becomes apparent when we model the impedance as a function of frequency. The result is a transfer function representation of the RLC network in the frequency domain[32].

Frequency response analysis is the response characteristics of the system when subject to sinusoidal inputs. The input frequency is varied, and the output characteristics are computed or represented as a function of the frequency. Frequency response analysis provides useful insights into performance characteristics of the system [6].

The system is subject to an input of the form

$x(t) = A\sin(\omega t)$

and the output is also a sinewave of the form

$y(t) = B\sin(\omega t + \phi)$

The amplitude and phase are changed by the system, but the frequency remains the same as shown in Figure 4.1. Output wave lags behind the input by an angle ϕ defined as the phase lag. Phase angle ϕ can be capacitive also and in that case it will be leading with respect to input signal. Similarly every time the frequency of the input signal is changed in a predefined interval ,keeping the amplitude to the input signal same constant value A and output signal is computed. In this process frequency is swept from low frequency to high frequency and this method is known as Sweep frequency response analysis (SFRA).

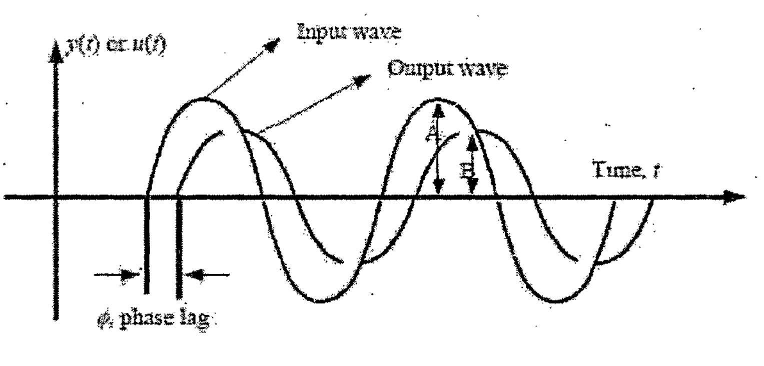

Figure 4.1: Frequency response of a sytem

There are a number of ways to represent the frequency response of a process and one of them is Bode plots. A Bode plot is a plot of the amplitude ratio (AR) and the phase lag as a function of the frequency of the input line wave (which is the same as the frequency of the output wave). Logarithmic scales are used for the frequency axis. The y-axis is

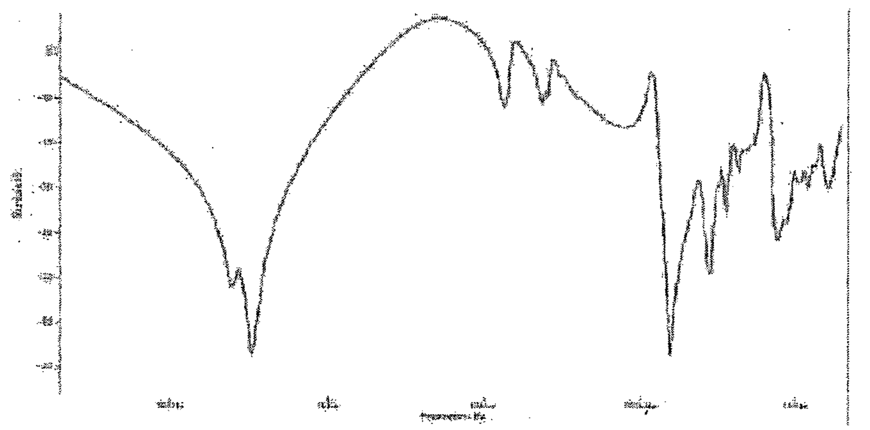

Figure 4.2: Logarithmic SFRA Plotting

plotted using the units of decibels, which is $20log(AR)$ as shown in Figure 4.2.

4.2.1 RLC Networks and Resonant Frequency

The series RLC circuit is mentioned in Figure 4.3 and the Frequency response plot of the series RLC circuit is shown in Figure 4.4. Parallel RLC circuit is mentioned in Figure 4.5.

For the Series RLC circuit the impedance (Z) is:

$$\mathbf{Z} = Z\angle\phi = R + j\left(\omega L - \frac{1}{\omega C}\right)$$

$$Z = \sqrt{R^2 + \left(\omega L - \frac{1}{\omega C}\right)^2}$$

$$\phi = \arctan\frac{\omega L - (1/\omega C)}{r}$$

At resonance of series or parallel circuit $\left(\omega L = \frac{1}{\omega C}\right)$ the resonant frequency f_0 is defined as below:

$$f_0 = \frac{1}{2\pi\sqrt{LC}}$$

Hence, at the resonant frequency the imaginary part of the impedance vanishes.

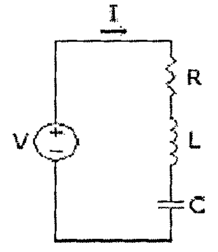

Figure 4.3: Series RLC circuit

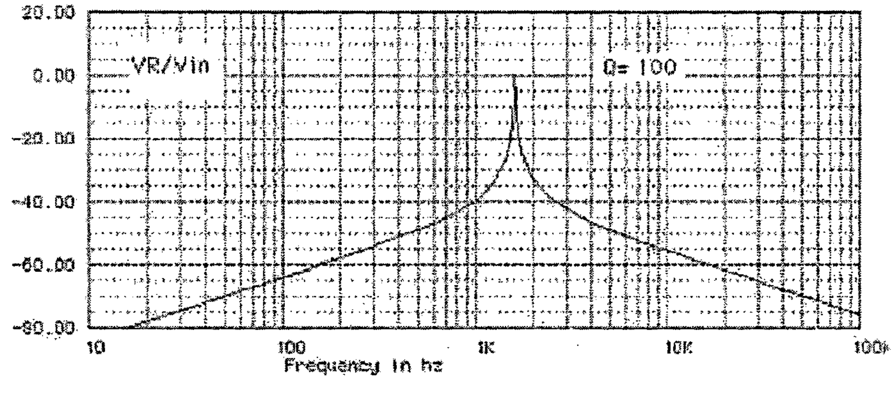

Figure 4.4: SFRA Plot for Series Resonance RLC circuit

Frequency response analysis is generally applied to a complex network of passive elements [8]. For practical purposes, we will only consider resistors, inductors, and capacitors as passive circuit elements, and they should be assumed ideal. These three fundamental elements are the building blocks for various physical devices, such as transformers, motors, generators, and other electrical apparatus.

It is important to understand the difference between the physical device and the mathematical model we intend to use. When large and complex systems are electrically analyzed, we are often faced with a poorly defined distributed network. A distributed network contains an infinite amount of infinitely small RLC elements. For example, transmission lines are generally distributed in nature. It is practical to model such distributed systems

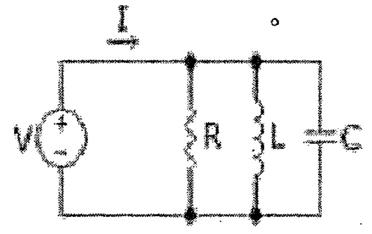

Figure 4.5: Parallel RLC circuit

by lumping the basic RLC components together, resulting in a lumped network. Lumping elements together for a single frequency is a easy task. However, when system modeling requires spanning over a significant frequency interval, then producing a suitable lumped model becomes difficult.

They can be connected in series, parallel or combination of series and parallel to produce the desired model. As the model increases in complexity, these forms can be combined.

4.2.2 Time and Frequency Domains

System responses can be represented either in the time domain or in the frequency domain and it is explained in reference [4]. Voltage and current signals can be observed over time, thus resulting in a signal versus time or time domain response. Any signal can be represented by a sum of harmonically related sinusoids, at varying magnitudes and phases. When a signal is represented by a sum of sinusoids, the result is displayed and represented in the frequency domain. Various tools and techniques can be applied in either case for analyzing the responses. Differential equations and convolutions are applied to nth order linear systems in the time domain, while Fourier and Laplace methods are used extensively for linear systems in the frequency domain.

The time domain and frequency domain are related collectively by the transform-pair relationship. Using the Fourier relationship as an example, the function $F(j\omega)$ is the Fourier transform of $f(t)$, and $f(t)$ is the inverse Fourier transform of $F(j\omega)$. The transform pair is defined by Equation 4.1.

$$F(j\omega) = \int_{-\infty}^{\infty} e^{j\omega} f(t)dt \Leftrightarrow f(t) = \frac{1}{2\pi}\int_{-\infty}^{\infty} e^{j\omega} F(j\omega)d\omega \tag{4.1}$$

The energy associated with f(t) is proportional to the energy associated with $F(j\omega)$.To better understand the relationship between the domains, the energy correlation should be examined closely. The energy of a signal can be represented by the sum of its individual orthogonal components, where inversely, the sum of such components, creates an equivalent time domain representation. The energy of a signal or system can be obtained by either $f^2(t)$ over time or by integrating $F^2(j\omega)$ multiplied by $1/(2\pi)$ over all frequencies.

This relationship is known as Parseval's theorem, which compares the total energy of a time domain system to a frequency domain system. Parseval's theorem is represented by Equation 4.2.

$$\int_{-\infty}^{\infty} f^2(t)dt = \frac{1}{2\pi}\int_{-\infty}^{\infty} |F(j\omega)|^2 d\omega \tag{4.2}$$

Often, it is difficult to analyze system responses displayed in the time domain, while the frequency domain equivalent may prove to be much easier. Identifying predominant system features, such as resonance, by time domain methods is not easily accomplished. When the same resonance is displayed using frequency domain techniques, the resonance characteristics are identified with clarity and confidence. Noise and harmonic content are other examples of where the frequency domain analysis is beneficial.

4.2.3 Two Port Networks

When a transformer is subjected to SFRA testing, the leads are configured in such a manner that four terminals are used. These four terminals can be divided into two unique pairs, one pair for the input and the other pair for the output. These terminals can be modeled in a two-terminal pair or a two-port network configuration as shown in Figure 4.6.

z_{11}, z_{22}, z_{12}, and z_{21} are the open-circuit impedance parameters, and can be determined by setting each current to zero and solving Equation 4.3.

$$\begin{bmatrix} V_1 \\ V_2 \end{bmatrix} = \begin{bmatrix} z_{11} & z_{12} \\ z_{21} & z_{22} \end{bmatrix} \begin{bmatrix} I_1 \\ I_2 \end{bmatrix} \tag{4.3}$$

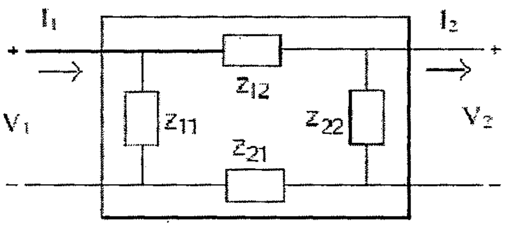

Figure 4.6: Two-Port Network

where

$z_{11} = \frac{V_1}{I_1}|_{I_2=0}$ $z_{12} = \frac{V_1}{I_2}|_{I_1=0}$ $z_{21} = \frac{V_2}{I_1}|_{I_2=0}$ $z_{22} = \frac{V_2}{I_2}|_{I_1=0}$

These impedances are formed by the complex RLC network of the specimen. It is assumed here that transformers are tested through the transformer tank. The transformer tank is common for both negative or lower terminals in figure 4.6. The transformer tank and lead ground shields must be connected together to achieve a common-mode measurement. This assures that no external impedance is measured. Applying the connection in this manner helps reduce the effects of noise. It is very important to obtain a zero impedance between the lower or negative terminals to assure a repeatable measurement.

4.2.4 Transfer Function

The transfer function of a RLC network is the ratio of the output and input frequency responses when the initial conditions of the network are zero. Both magnitude and the phase relationships can be extracted from the transfer function. The transfer function helps us better understand the input/output relationship of a linear network. The transfer function also represents the fundamental characteristics of a network, and is a useful tool in modeling such a system The transfer function is represented in the frequency domain and is denoted by the Fourier variable $H(j\omega)$, where $(j\omega)$ denotes the presence of a frequency dependent function. The Fourier relationship for the input/output transfer function is given by Equation 4.4.

$$H(j\omega) = \frac{V_{output}(j\omega)}{V_{input}(j\omega)} \tag{4.4}$$

When a transfer function is reduced to its simplest form, it generates a ratio of two polynomials. The main characteristics, such as resonance, of a transfer function occurs at the roots of the polynomials. The roots of the numerator are referred to as "zeros" and the roots of the denominator are "poles". Zeros produce an increase in gain, while poles cause attenuation. The goal of SFRA is to measure the impedance model of the test specimen. The Bode Diagram plots the magnitude and phase as follows:

$$A(dB) = 20log_{10}(H(j\omega))$$
$$A(\theta) = \tan^{-1}(H(j\omega))$$

The Bode Diagram takes advantage of the asymptotic symmetry by using a logarithmic scale for frequency. The Bode method is the effective way to estimate a transfer function. The frequency scale is plotted by decades, such as 1, 10, 100, 1k, 10k, etc. The effect of poles and zeros are very unique to the Bode Diagram. Poles and zeros create a 20 dB per decade change for a single root.

Poles cause -20 dB per decade deficit, while zeros produce a gain of -20 dB per decade.Plotting the phase relationship with the magnitude data will help determine whether the system is resistive, inductive, or capacitive. It is often useful to compare resonance in the magnitude plots with the zero crossings in the phase relationship. It is more advantageous to plot H(s) logarithmically over large frequency spans. The Logarithmic plot helps to maintain consistent resolution. Plots ranging from 10 Hz to 2 MHz can be displayed as a single plot if they are formatted logarithmically. However, when zooming in closely, a linear plot may help to simplify the plot interpretation in high frequency by having evenly spaced frequency scale. Figure 4.2 and Figure 4.7 compares a logarithmic plot to a linear plot over a substantial frequency range for the same measurement.

The measured response is usually shown graphically by plotting the logarithmic amplitude ratio of the output voltage to the input voltage in dB (y scale) against the frequency (x scale). The frequency scale can be logarithmic or linear. Both are used, although the logarithmic often shows the complete frequency range more clearly. The linear scale is useful for looking at discrete frequency bands and to compare small differences at particular frequencies.

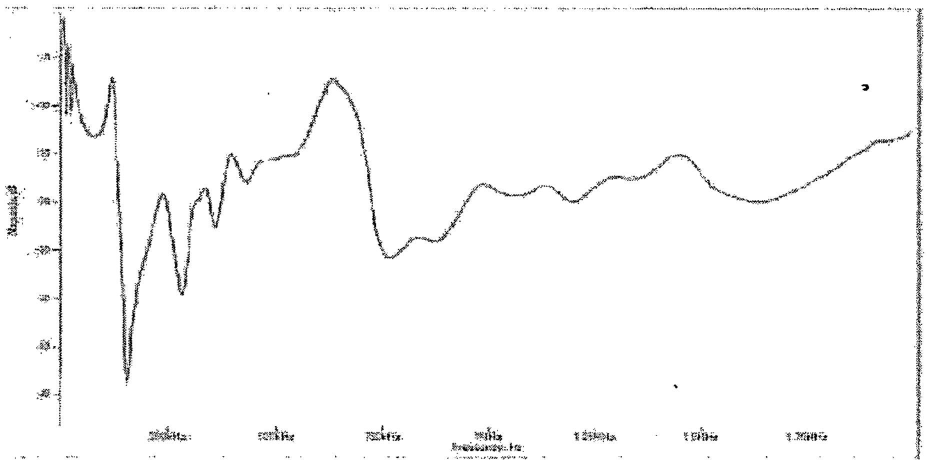

Figure 4.7: Linear SFRA Plotting

4.3 Application of SFRA in Power Transformers

Power transformers are specified to withstand the mechanical forces arising from both shipping and subsequent in-service events, such as faults and lightning. Transportation damage can occur if the clamping and restraints are inadequate; such damage may lead to core and winding movement. The most severe in-service forces arise from system faults, and may be either axial or radial in nature. If the forces are excessive, radial buckling or axial deformation can occur [49]. With a core form design the principal forces are radially directed, whereas in a shell form unit they are axially directed, and this difference is likely to influence the types of damage found.

Once a transformer has been damaged, even if only slightly, the ability to withstand further incidents or short circuits is reduced. There is clearly a need to effectively identify such damage. A visual inspection is costly and does not always produce the desired results or conclusion. During a field inspection, the oil has to be drained and confined space entry rules apply. Since so little of the winding is visible, often little damage is seen other than displaced support blocks. Often, a complete tear down is required to identify the problem. An alternative method is to implement field-diagnostic techniques that are capable of detecting damage, such as SFRA [41].

There is a direct relationship between the geometric configuration of the winding and core within a transformer and the distributed network of resistances, inductances, and capacitances parameter of transformer as shown in Figure 4.8. This RLC network can be identified by its frequency dependent transfer function[6].Changes in the geometric configuration alter the impedance network, and in turn alter the transfer function. Changes in the transfer function will reveal a wide range of failure modes. SFRA allows detection of changes in the transfer function of individual windings within transformers and consequently indicate movement or distortion in core and windings of the transformer.

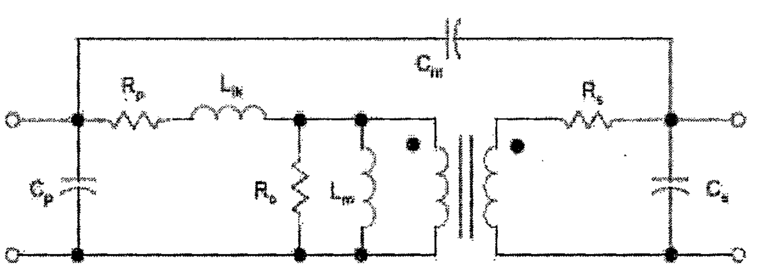

Figure 4.8: Equivalent circuit model for two winding Transformer

Where

L_{1k}= Primary inductance

L_m = Leakage inductance

C_p = Primary winding capacitance

C_s = Secondary winding capacitance

C_m = Inter winding capacitance

R_p = Primary winding resistance

R_s = Secondary winding rèsistance

4.3.1 Self Inductance

From Maxwell's first equation (on integral form) we may obtain the magnetic contribution along a circular loop carrying current (due to the applied electrical field)

$$\oint \vec{E} \cdot \vec{ds} = -\frac{\partial \phi}{\partial t} = \frac{\partial}{\partial t} \int \int \vec{B} \cdot \vec{n} dA = -\frac{\partial}{\partial t} \oint (\vec{A} \cdot \vec{ds}) \quad (4.5)$$

Assuming $\vec{B}$ is proportional to $\vec{H}$ (only linear materials) the flux through the loop is proportional to the total current carried by the loop. The proportionality is described by the self inductance of this loop. Assuming the loop is placed in vacuum (no ferromagnetic materials included), the inductance of the loop is depending on its geometry only. The total flux through the loop is expressed as:

$$\phi = \int\int(\vec{B} \cdot \vec{n})dA = \oint(\vec{A} \cdot \vec{ds}) = L \cdot I \tag{4.6}$$

In the latter only the external inductance is considered, due to the fact that the internal inductance is depending on the current distribution within the conductor (which in turn is determined by the skin-effect/frequency). For a circular conductor the flux through the loop is determined by:

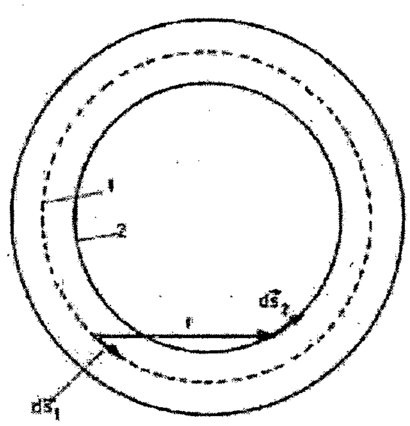

Figure 4.9: Integration paths to find self inductance

$$\phi = \phi_{outer} = \oint_{c2}\left[\frac{\mu_0 \cdot I}{4\pi}\oint_{c1}\frac{\vec{ds_1}}{r}\right] \cdot \vec{ds_2} = \frac{\mu_0 \cdot I}{4\pi}\oint_{c1}\oint_{c2}\frac{\vec{ds_1} \cdot \vec{ds_2}}{r} \tag{4.7}$$

and then:

$$L = L_{outer} = \frac{\mu_0}{4\pi}\oint_1\oint_2\frac{\vec{ds_1} \cdot \vec{ds_2}}{r} \tag{4.8}$$

The two paths of integration to find the inductance is shown in Figure4.9, where $\vec{ds_1}$ the unity vector quantity along the centre-line of the loop, and $\vec{ds_2}$ is the unity vector along a closed curve on the surface of the conductor .

4.3.2 Mutual Inductance

Mutual inductance is calculated using the same approach as the initial considerations for self inductance, where the mutual inductance between two parallel conducting filaments is calculated. This integral can be expressed as:

$$M_{12} = \frac{\mu_0}{4\pi} \int_0^{2\pi} \int_0^{2\pi} \frac{r_1(\alpha_1) \cdot r_2(\alpha_2) \cdot \cos(\alpha_1 - \alpha_2)}{R_{12}(\alpha_1 \cdot \alpha_2)} d\alpha_1 d\alpha_2 \tag{4.9}$$

The integral is also used for calculating the inductances of deformed/buckled windings. The approach, by assuming filaments of negligible cross-section, is rather coarse if the dimensions of the cross-section are appreciable compared to the distance d, between the filaments as indicated in Figure 4.10 and Figure 4.11.

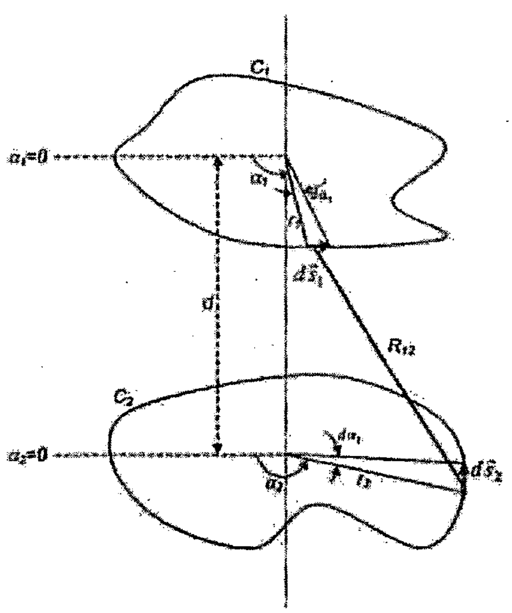

Figure 4.10: Two parallel conducting filaments

4.3.3 Series Capacitance

There are several types of windings but some of the main types of windings are listed here:

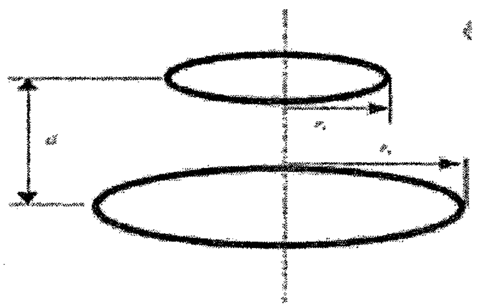

Figure 4.11: Mutual coupling between two circular filaments

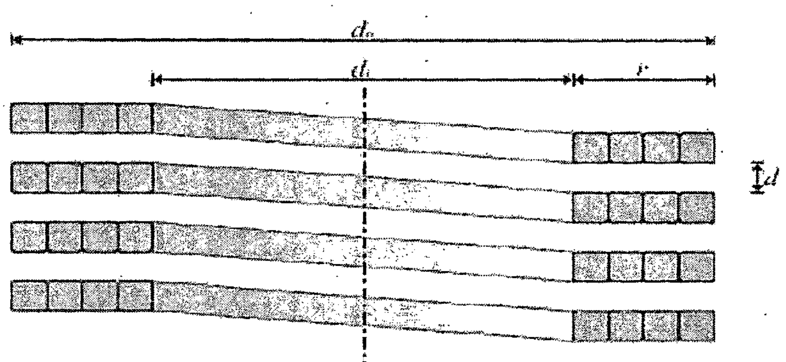

Figure 4.12: Helical winding (single layer, single-start)

- Helical winding (single- or multi-layer)
- Disc winding (conventional, interleaved or in-wound shields)
- Layer winding (conventional or interleaved)

Helical winding is shown in Figure 4.12 and the equation for computing the series capacitance is mentioned below.

$$\acute{C}_s = \epsilon_r \epsilon_0 \pi \frac{\acute{d}_o^2 - \acute{d}_i^2}{4d} \tag{4.10}$$

Where

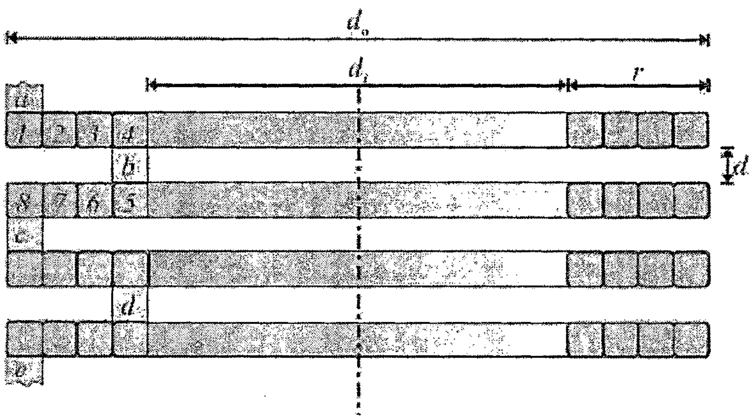

Figure 4.13: Ordinary (continuously wound) disc winding

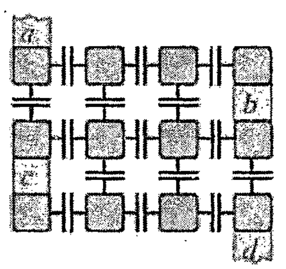

Figure 4.14: Equivalent circuit for disc winding

d: distance between turns.

$\acute{d}_o := d_o + d$: outer diameter + interturn distance (accounting for fringing)

$\acute{d}_i$: inner diameter - distance between turns.

The series capacitance for the whole winding is:

$$C_s = \frac{1}{n_t - 1}\acute{C}_s \tag{4.11}$$

Where

n_t: number of turns

For conventional disc windings is shown in Figure4.13, and the related capacitance of the winding is explained in Figure 4.14.

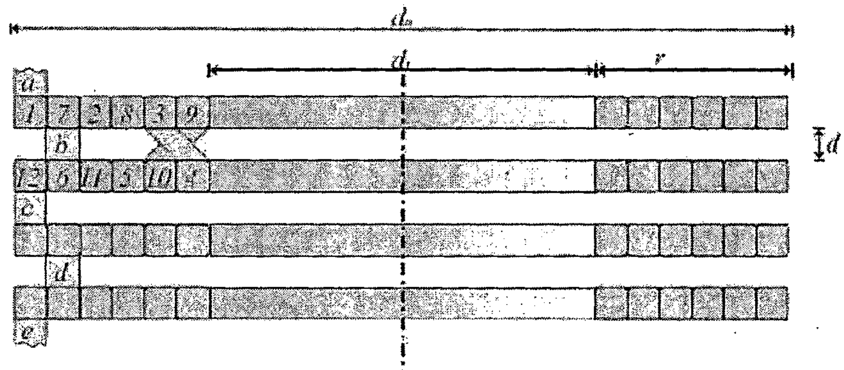

Figure 4.15: Interleaved disc winding

In Figure 4.15, an interleaved disc winding is shown. There are also other possibilities of interleaving, such as a 4 disc interleaving, but then the voltage between strands will be higher.

4.3.4 Shunt capacitance

These are capacitances between windings and between winding and ground. Some of these values are calculated with simplified geometrical formulas, and some are calculated on a semi-empirical basis.

Capacitance between windings where the windings are concentrically arranged around the core and can be treated as cylindrical capacitors given by:

$$C_g = \frac{2\pi\epsilon_r\epsilon_0 h'}{\ln\left(\frac{d_i}{d_o}\right)} \tag{4.12}$$

where h' = h+d is to compensate for fringing of the field at the ends, di is the inner diameter and d0 is the outer diameter, d is the distance between them as indicated figure 4.16.

Capacitance between phases: The following formula applies for capacitance between

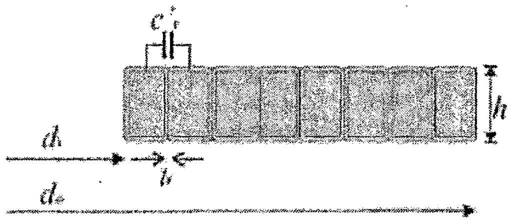

Figure 4.16: Dimensions of a single disc

windings on adjacent legs,

$$C_p = \frac{\epsilon_r \epsilon_0 \pi h'}{\ln\left(\frac{b}{d_o} + \sqrt{\left(\frac{b}{d_o}\right)^2 - 1}\right)} \tag{4.13}$$

where b is the distance between adjacent windings (centre-centre) and d_o is the diameter of the windings as indicated in Figure 4.17.

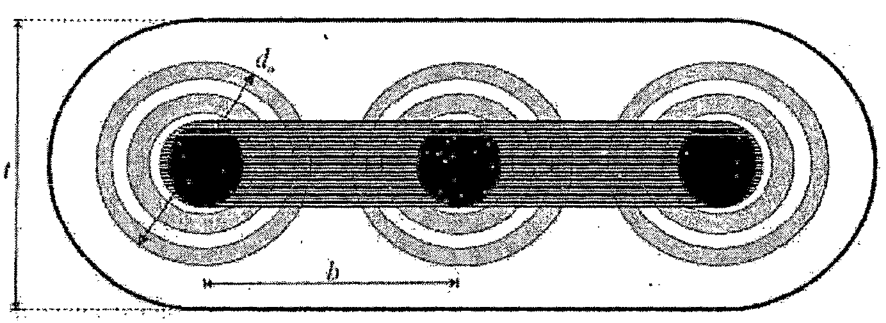

Figure 4.17: Dimensions between adjacent windings and between windings and tank

Capacitance between phase and the tank: The capacitance between centre phase and the tank for the winding configuration shown in Figure 4.17, is calculated as mentioned below.

$$C_t = 0.25 \cdot \frac{\epsilon_r \epsilon_0 \pi h'}{\ln\left(\frac{t}{d_o} + \sqrt{\left(\frac{t}{d_o}\right)^2 - 1}\right)} \tag{4.14}$$

4.3.5 Low and High Frequency model

Equivalent circuit of transformer when considered for low frequency application, is represented by leakage inductance, winding resistance and series inductance as represented in Figure 4.18.

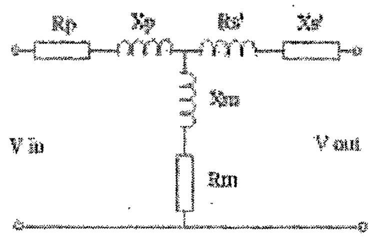

Figure 4.18: Equivalent circuit of Transformer winding at Low frequency

The same is different when considered in high frequency applications as shown in Figure 4.19. An element of capacitance becomes dominant as frequency increase and it is because of its reactance which is inversely proportional to the frequency.

As the frequency increases, the capacitance between successive coils of the windings and the coupling between them becomes more dominant. Thus a more accurate model for higher bandwidth operations would include capacitance of the primary winding, capacitance of the secondary winding and a capacitance representing the coupling between the primary and secondary windings. The inductive reactance of both windings increases with frequency and become a high impedance in parallel with the capacitive reactance of the windings as shown in Figure 4.19.

Thus for more higher frequencies it is the LC circuit which is more sensitive than mere L alone as shown in Figure 4.20. Elements Inductance L and capacitance C are mainly Geometry dependant. They are governed by dimensions; height, diameter, Length, width and thickness. For transformer windings, once made these parameters like inductance formed by number of turns and dimensions , capacitance between turns or discs, between windings, between leads remains constant for years together unless changed by external forces, such as electromagnetic forces due to short circuit currents in winding, shocks while transports or insulation failures.

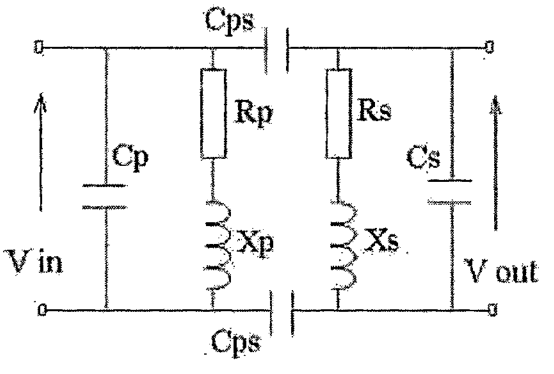

Figure 4.19: Equivalent circuit of Transformer winding at high frequenncy

As it is mentioned above that the LC circuit is very sensitive to frequency, the benefit of this sensitivity is efficiently used in a technique called Sweep Frequency Response Analysis SFRA. Any $L-C$ circuit has its own frequency vs Impedance characteristic. In other words, for a given LC circuit if the frequency vs impedance characteristics change from its initial characteristics then it is only due to some change in values of L and C and any change in L and C means a change in their dimensions if other parameters such as permittivity and permeability remains constant which is normally true for equipment like power transformer.

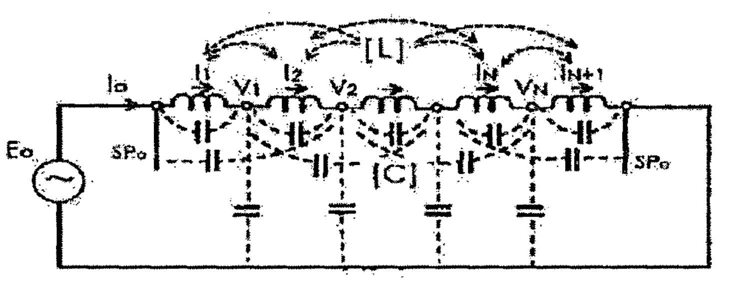

Figure 4.20: Model LC Circuit for very high frequency response

4.4 Methods of SFRA Measurement

4.4.1 Voltage Transfer Measurement:

The transformer winding can be regarded as a passive, linear two-port network composed of resistance, inductance and capacitance. After the deformation of windings the parameters, mainly the inductance and the capacitance, have a change and so does the performance of the network. The changes of transfer function can be adopted as the criterion of the winding deformation.

Connections of the instrument to the transformer using three coaxial test leads are as shown in Figure 4.21. It can be seen from the diagram that the swept frequency sinusoidal signal output (S) of approximately 10 V_{pp} from the measurement unit of the Analyzer and one measuring input (R) are connected to the one end of a winding, while the other end of the winding is connected to the other measuring input (T). The voltages are applied and measured with respect to the earthed transformer tank.

The voltage transfer function T/R is measured for each winding for standard frequency scans from $10Hz$ to $2MHz$, and amplitude and phase shift results are recorded for subsequent analysis [42].

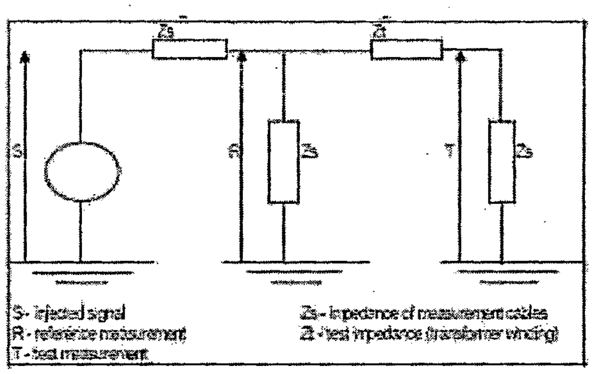

Figure 4.21: Basic circuit for SFRA measurement

It is ensured that the winding which is not under test is terminated in open condition in order to avoid response difference among the three phases. The same procedure is followed on subsequent tests on the same or similar transformer, to ensure that measurements are entirely repeatable. The voltage transfer function is measured for each winding as indicated in Figure 4.22.

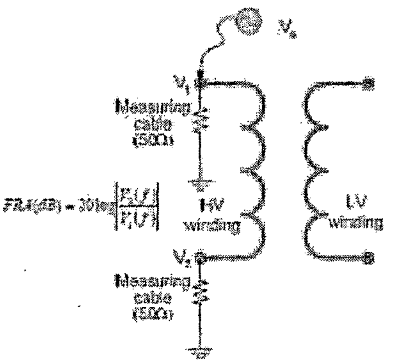

Figure 4.22: Parameters to be measured for SFRA

Winding measurements realistically consist of five categories. The winding categories are high-voltage, low voltage, inter-winding , series, and common. Inter-winding measurement is not a true winding measurement, but rather the transfer impedance between two windings. The series and common winding measurements describe the SFRA application as it is applied to auto-transformers. Regardless, certain expectations can be made for each.

These five measurement types produce a few predictable characteristics and properties .Understanding these properties will minimize measurement error and identify problems. The following features exist for each of the following categories.

4.4.1.1 High-Voltage Winding

High-voltage winding measurements have greatest attenuation as compared to the other categories. Most traces start between -30 dB and -50 dB and are initially inductive. High-voltage windings are much larger in overall size, which contributes to greater complexity in its distributive network. High-voltage winding measurements generally produce steeper resonances and more of them as compared to its low voltage counterpart. Figure 4.23 illustrates these features.

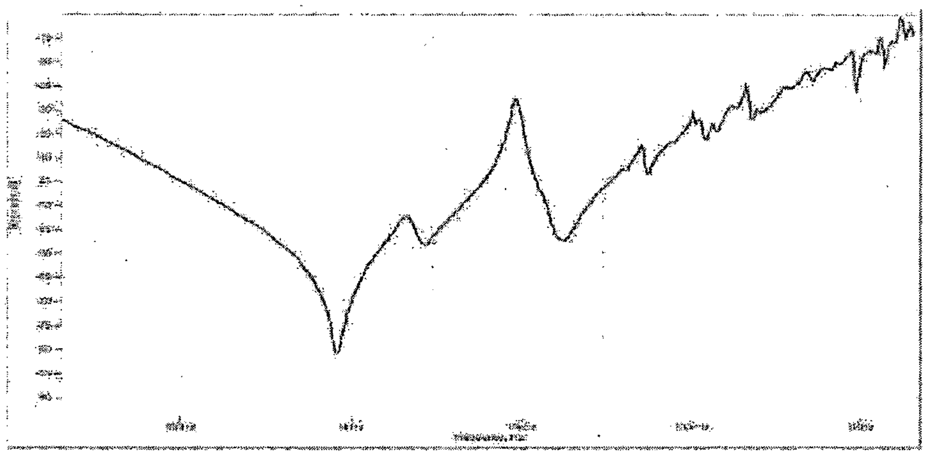

Figure 4.23: HV winding plot

4.4.1.2 Low-Voltage Winding

Low-voltage winding measurements have least attenuation as compared to the other categories. Most traces start between $-5dB$ and $-15dB$ and are also initially inductive. This characteristic is due to the low impedance property of the LV winding of the transformer. The first peak after the core resonance generally approaches $-5dB$ to $0dB$ and is concave and smooth. As compared to the high-voltage winding response, the low-voltage winding has fewer fluctuations and is slightly smoother. Figure 4.24 illustrates these features.

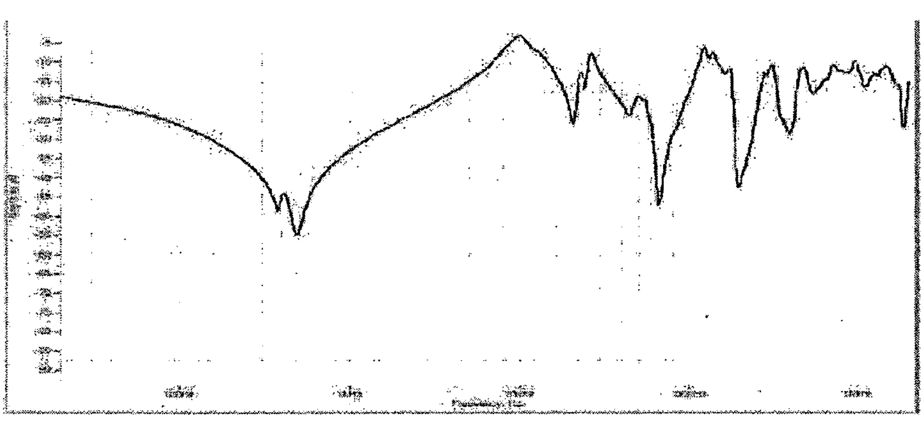

Figure 4.24: LV Star winding plot

4.4.1.3 Inter-Winding

Inter-winding measurements always start with high attenuation, between $-60dB$ and $-90dB$, and are capacitive. If electrostatic interference is present, it will show up$50Hz$ and at the associated harmonics of $50Hz$ during this measurement. These traces are very common, most inter-winding traces adhere to one of the basic shapes shown in Figure 4.25. It should be noted that inter-winding measurements, are capacitive in nature at low frequency.

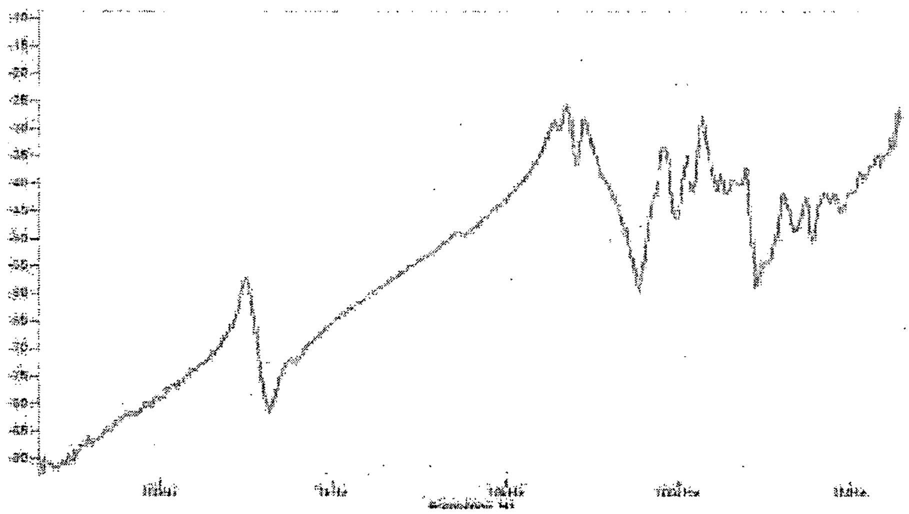

Figure 4.25: Inter winding plot of 132 kV/33 kV Transformer

4.4.1.4 Series and Common Winding

The series and common winding measurements are grouped together because of their similarities. These measurements are associated with auto-transformer. The naturally low turns ratio of an autotransformer cause the series and common measurements to be similar. However, if a LTC is associated with either winding, the similarities will be somewhat jeopardized. The common winding always exhibits less attenuation then the series winding. Figure 4.26 illustrates these features, and were obtained from a 440MVA 345 kV/138 KV auto-transformer.

The lower resonant frequencies for the series winding are due to the fact that the interleaved disc series winding has a higher values of series capacitance than both the

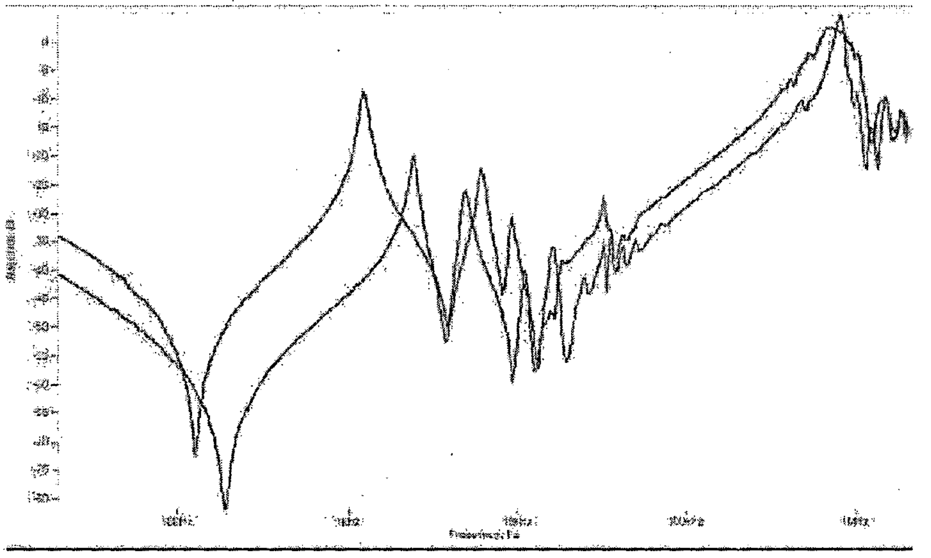

Figure 4.26: Series (blue) and Common winding (red) plot of Auto Transformer

common and tertiary windings.

4.4.2 Impedance Measurement

It is the same measurement as the voltage transfer method and indicates the effect of frequency variation on impedance of a winding due to its inter-turn and ground capacitance, self and matual reactance as indicated in Figure 4.27.

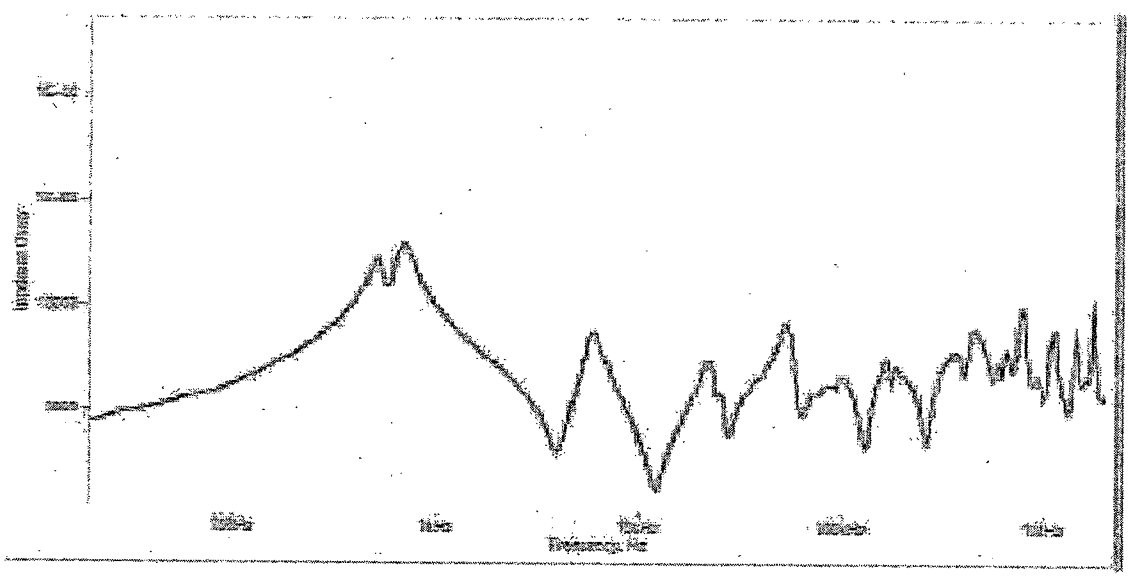

Figure 4.27: Impedance plot of LV winding